metals

MDPI

Article

Investigation on a Novel Laser Impact Spot Welding

Huixia Liu *, Shuai Gao, Zhang Yan, Liyin Li, Cong Li, Xianqing Sun, Chaofei Sha, Zongbao Shen, Youjuan Ma and Xiao Wang

School of Mechanical Engineering, Jiangsu University, Zhenjiang 212013, China; gaoshuai2017@163.com (S.G.); yz@ujs.edu.cn (Z.Y.); llyliliyin@163.com (L.L.); Licong183@126.com (C.L.); xianqingyzy@163.com (X.S.); shachaofei@gmail.com (C.S.); szb@ujs.edu.cn (Z.S.); myj@ujs.edu.cn (Y.M.); wx@ujs.edu.cn (X.W.)

* Correspondence: lhx@ujs.edu.cn; Tel.: +86-511-8878-0276; Fax: +86-511-8878-0276

Academic Editor: Patrice Peyre

Received: 29 June 2016; Accepted: 28 July 2016; Published: 3 August 2016

Abstract: In this paper a novel laser impact spot welding (LISW) method is described, in which a hump was formed on the flyer plate on the intended welding spot location by local pre-forming. When the flyer and base plates were placed together to perform welding, the two plates kept in contact over their entire surfaces except at the hump, where a local air gap was enough to guarantee the impact velocity and collision angle to achieve spot welding using laser pulse energy. The presented approach was implemented to join thin titanium foils to copper foils under low laser energy system. Joints with regular shapes were obtained. The microstructure in the weld interface was studied with scanning electron microscopy (SEM) and energy dispersive spectroscopy (EDS). It was found that the jetting occurred at the central region of the weld spots due to oblique impact. Wave features were observed in the weld interfaces. The impact energy was found to have significant influence on the wave's characteristics. Moreover, SEM images and EDS analysis did not show apparent element diffusion across the weld interface. Besides, the lap shearing test was used to characterize the mechanical properties of the spot welded joints.

Keywords: laser impact spot welding; wavy interface; jet formation; lap shearing test; laser impact welding

1. Introduction

It is well known that titanium (Ti) has the properties of high strength-to-weight ratio and high temperature creep resistance, and copper (Cu) combines excellent performances of high thermal and electrical conductivity. Joining titanium to copper would provide a material with light weight and high strength and meet the requirements of heat and electrical conduction, thus having broad application prospects in industries [1,2]. Joining of titanium and copper has therefore been of great significance and interest. In order to obtain a reliable Ti/Cu joint, applying a reliable joining technique is essential. However, fusion welding and brazing welding are not suitable for joining Ti to Cu because brittle Ti–Cu intermetallic compounds (IMCs) are easily formed [3–5], which can seriously cause the mechanical properties of the Ti/Cu joint to deteriorate. Therefore, several kinds of welding techniques, such as explosive welding [6], friction welding [7], diffusion welding [8], and vaporizing foil actuator welding [9] were presented as methods for joining Ti to Cu plates. In recent years, with the rapid development of microelectronics and medical industries, joining of thin Ti foil to Cu foil may have a wide application prospect. Due to its small thickness and length values relative to of the parts involved, however, the methods mentioned above may have some limitations.

Laser impact welding (LIW) is a relatively novel solid state joining process patented by G.S. Daehn and J.C. Lippold [10], in which two metal plates were joined at low temperature under elevated impact velocity and collision angle. It shares the impact-driven solid state welding mechanism with explosive welding (EXW) [11], magnetic pulse welding (MPW) [12], and vaporizing foil actuator

welding (VFAW) [13]. However, unlike these techniques, LIW utilizes laser induced shockwave as the driving force to accelerate the flyer plate. The feasibility of laser impact welding was previously presented by Zhang et al. [14] and Wang et al. [15]. Zhang et al. [14] studied the welding of 50 μm thick aluminum alloy 1100 and low carbon steel block. Wave interface was observed. Wang et al. [15] then investigated three kinds of geometric arrangements of the base plates by means of LIW. Results showed that welding did not occur at a relatively large angle (30°) with corrugate base plate. In other words, their research indicated that the LIW technique is suitable for joining dissimilar metal foils with small thickness and length values, and does not depend on the electrical conductivity of the flyer plate compared with EXW and MPW. This makes the method promising for applications in the manufacture and assembly of micro-devices, such as medical devices [14].

Therefore, joining of dissimilar metal foils utilizing LIW has been of interest over the past three years. Wang et al. [16] discussed the welding ability of aluminum/copper foils. The impact angle was 20°, which is the tapered angle on back support as shown in Figure 1a. They observed two different interface morphologies, and claimed that the increase of the interfacial hardness was mainly due to the local plastic deformation caused by oblique impact. Afterwards, Wang et al. [17] presented the laser impact spot weld process shown in Figure 1b and welded the Al and Cu metal foils. The effect of standoff distances on the dimensions and the surface morphologies of the weld spots were discussed. Similar to the aforementioned research, wave interfaces were also observed. More recently, Wang et al. [18,19] reported the welding of Al/Ti with LIW and did not observe intermetallic phases in the weld interface.

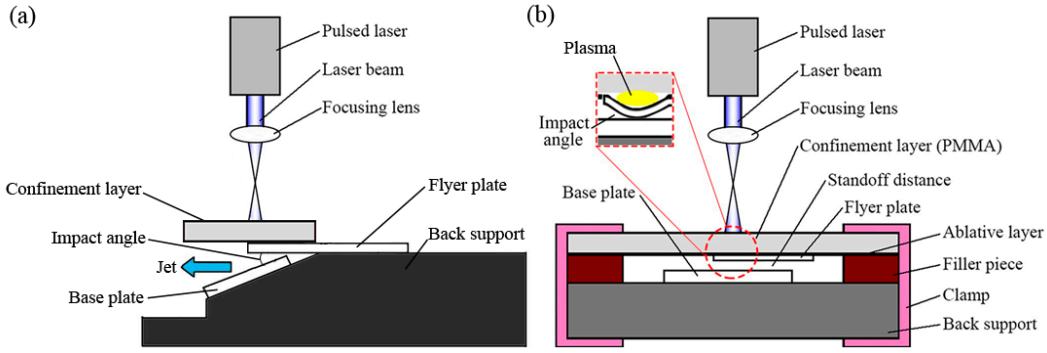

Figure 1. Schematic diagram of laser impact welding: (**a**) angle welding [16]; (**b**) parallel welding [17].

Two basic geometric configurations of the LIW process have been reported, including angle welding [14,16] and parallel welding [17–19] as shown in Figure 1. However, in the angle welding process, the collision angle is constructed by means of an experimental device as shown in Figure 1a, which makes the clamping of the flyer plate and the base plate complicated. Thus, the efficiency of welding may be greatly affected. In the parallel welding process shown in Figure 1b, connection between the flyer plate and the base plate is required with cyanoacrylate adhesive or double-sided sticky tape. However, there can be reduced reproducibility. Additionally, a connecting layer remaining on the weld spots is difficult to clear up after LIW, especially when cyanoacrylate adhesive is used. Thus, the quality of the weld spots is difficult to guarantee. These defects may limit the application of LIW in the manufacture and assembly of micro-devices. Moreover, a certain standoff distance is required between the flyer plate and the base plate in the above two approaches, which also can make LIW difficult to be applied in microelectronics and medical industries. So, it is meaningful to improve the LIW process.

Therefore, the goal of the present study was to improve LIW technique by overcoming these limitations. A new laser impact spot welding (LISW) approach is presented and applied to join thin titanium foil to copper foil with a low laser energy system. The morphology of the weld spots was

examined and the microstructure in the weld interface was studied. Finally, the bonding strength and failure mode of the joint were investigated by lap shearing test.

2. Mechanism of Laser Impact Spot Welding

Figure 2 schematically illustrates the basic concept of LISW. The experimental setup consists of blank holder, confinement layer, ablative layer, flyer plate, base plate, double sided sticky tape, spacer, and back support. The blank holder with 12 N blank holder force was used to prevent the leakage of the plasma induced by laser pulse energy. Polymethyl methacrylate (PMMA) with a thickness of 3 mm was selected as the confinement layer. A thin layer of black lacquer with a thickness of about 10 μm was chosen as the absorbing layer and painted on the surface of the hump on the flyer plate. The flyer plate was fixed on the base plate with black tape. The base plate was fixed on the back support with double-sided sticky tape. A spacer was used to support the confinement layer.

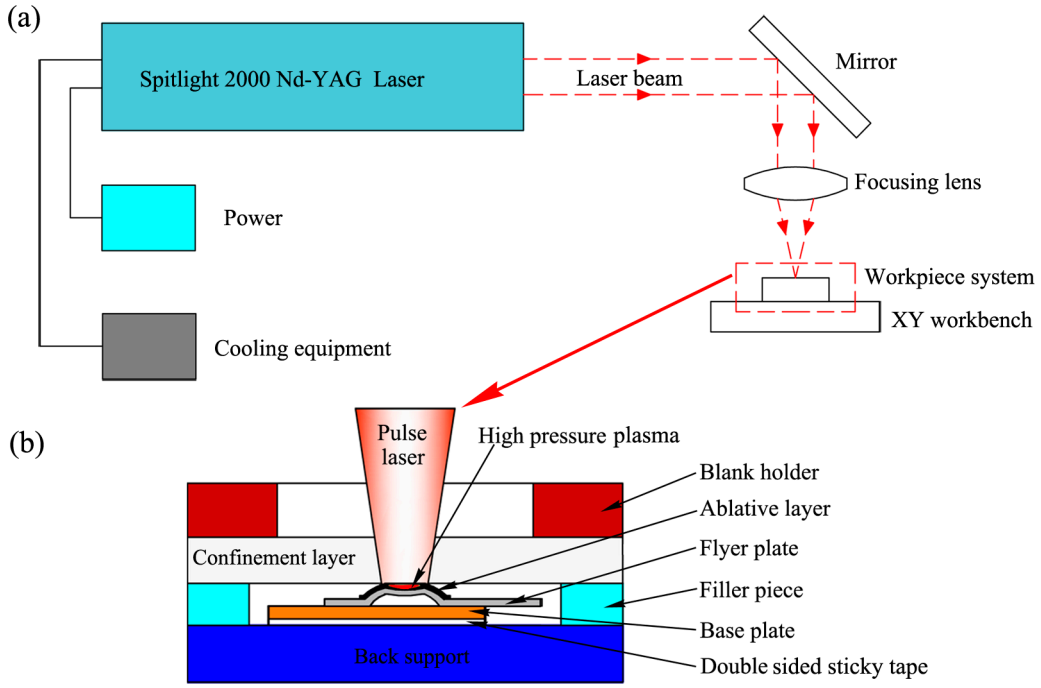

Figure 2. (**a**) The welding system of laser impact spot welding; (**b**) experimental principle of laser impact spot welding.

As shown in Figure 2b, a hump was formed on the flyer plate at the intended spot welding location by local pre-forming. When two plates were placed together to perform welding, the plates kept in contact over their entire surfaces except at the hump, where a local air gap was big enough to guarantee the impact velocity and collision angle to obtain spot welding using laser pulse energy. The mechanism behind this process is the same as LIW, and the bonding process can be described as follows: when an intense laser pulse passes through the transparent confinement layer and irradiates onto the ablative layer, the absorbent material vaporizes instantaneously and forms a high-temperature and high-pressure plasma. The plasma continues to absorb the laser energy. The rapidly expanding plasma is confined by the transparent confinement layer, and creates a high surface pressure, which propagates into the hump as a shockwave [20,21]. The shockwave drives the hump to impact onto the base plate at a high speed. A jet is expected to be generated, which will remove the oxidized surface layer and produce two fresh surfaces by the oblique impact. Then solid state bonding can be obtained under the great impact pressure and plastic shear deformation in the interface [22–25]. The whole process is completed in microseconds [14]. The air gap is determined by the dimensions of the hump. The impact velocity of the hump is affected by laser pulse energy.

3. Experimental Materials and Equipment

3.1. Experimental Materials

The sample materials used in this study were pure titanium (TA2) foils 0.03 mm in thickness and pure copper (T2) foils 0.10 mm in thickness. They were selected as flyer and base plates, respectively. The chemical compositions of the titanium foil and copper foil are listed in Tables 1 and 2, respectively. The copper foils were annealed at 673 K for 2 h to obtain a fine grain structure [17]. The flyer and base plates were cut into rectangle with dimensions of 20 mm × 3 mm and 20 mm × 20 mm, respectively. Prior to welding, the sample surfaces were slightly polished using sand paper with a roughness of 3000 and then cleaned with anhydrous alcohol.

Table 1. Chemical composition of titanium (TA2) (wt. %).

Elements	C	Fe	N	H	O	Ti	Other
titanium	0.1	0.30	0.005	0.015	0.25	Bal.	0.01

Table 2. Chemical composition of copper (T2) (wt. %).

Elements	Cu + Ag	Bi	Sb	As	Fe	Pb	S	Other
Copper	99.9	0.001	0.002	0.002	0.005	0.005	0.005	0.01

According to the basic principle of LIW, a standoff distance between the flyer plate and base plate is required to ensure enough high impact velocity and an appropriate dynamic collision angle to complete welding. In the present study, the air gap was fixed to 0.20 mm through local pre-forming performed at the intended welding spot location on the flyer plates as shown in Figure 3. Figure 3a presents the location of the hump on the flyer plate. Figure 3b displays the cross-section configuration of the hump.

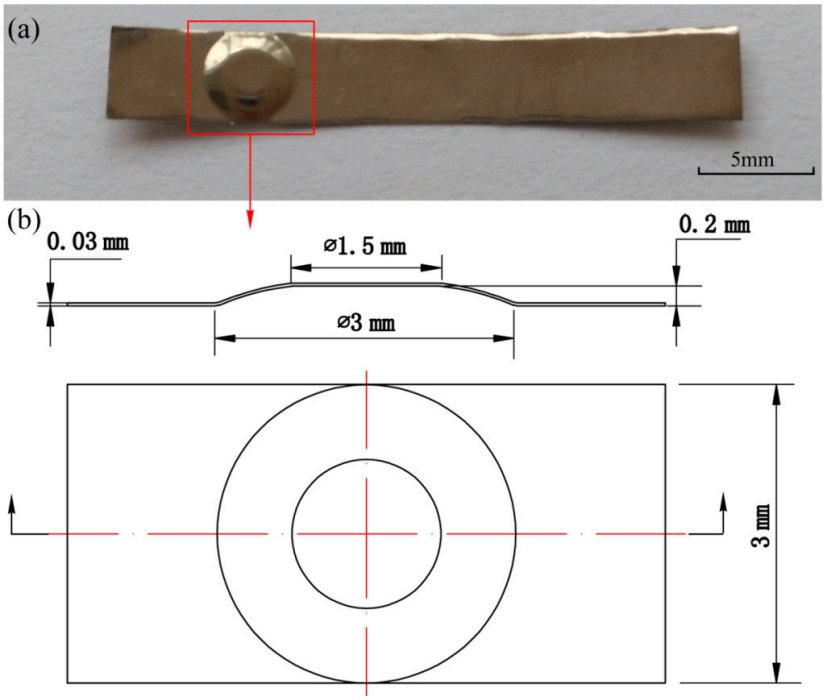

Figure 3. The design of the hump on the flyer plate: (**a**) location of the hump on the flyer plate; (**b**) cross-section configuration of the hump.

3.2. Experimental Equipment

The LISW experiments were carried out using a Spitlight 2000 Nd:YAG laser (InnoLas Corporation, München, Germany) with a Gaussian distribution beam. And its main parameters were listed in Table 3. A three-axis motion system was used to control the relative position between the laser beam and the intended welding location. Some key experimental conditions are listed as follows in Table 4.

Table 3. Main parameters of Spitlight 2000 Nd:YAG Laser.

Parameters	Values
Pulse energy	80–1800 mJ
Wave length	1064 nm
Pulse width	8 ns
Energy stability	$<\pm 1\%$
Exit spot diameter	9 mm

Table 4. Detailed experimental conditions and specimen parameters.

Parameters	Values
Materials (flyer/base)	Ti/Cu
Flyer plate thickness (mm)	0.03
Base plate thickness (mm)	0.1
Laser spot size (mm)	1.6
Laser pulse energy (mJ)	565, 835, 1200, 1550

After the LISW experiment, samples were cleaned with anhydrous alcohol to remove the remaining black lacquer on the surface of the weld spots. The samples used for the welding interface morphology and microstructure investigation were cut from the edge of weld spots and fixed with a cold inlaid technique, and then subjected to standard metallographic preparation procedures. The surface morphology and cross-sections of the spot welded Ti/Cu joints were examined by a KEYENCE VHX-1000C microscope (KEYENCE Corporation, Osaka, Japan) with a depth-of-field and resolution. The microstructure of the Ti/Cu weld interface was observed using a scanning electron microscopy (SEM, Hitachi Corporation, Tokyo, Japan) equipped with an energy dispersive spectroscopy (EDS, EDAX Corporation, Mahwah, NJ, USA). Lap shearing tests were carried out at room temperature using Instron Type UTM 4104 testing machine (SUNS Corporation, Shenzhen, China) at a speed of 2 mm/min, according to the EN ISO 527-1:2012 standard [26]. The tests were performed three times for each condition (565 mJ, 835 mJ, 1200 mJ, and 1550 mJ pulse energy).

4. Results and Discussion

4.1. Weld Examples

Titanium and copper plates were all successfully welded with four kinds of pulse energies. Figure 4 shows the weld samples and weld spots morphology of Ti/Cu joints produced at different pulse energies. It can be seen that the shape of the weld spots was regular compared with the previous reports [16,17]. This may be because the plates remained in contact over their entire surfaces—except at hump—and only local plastic deformation occurred on the hump during LISW. Springback can also be observed in the center of the weld spot as shown in Figure 4a; the area of the springback region increased when high pulse energy was used, as shown in Figure 4b. A similar phenomenon has been observed elsewhere [17,19]. The occurrence of the springback may be related to the effect of the reflected shockwave. Research from Wang et al. [17] confirmed the same.

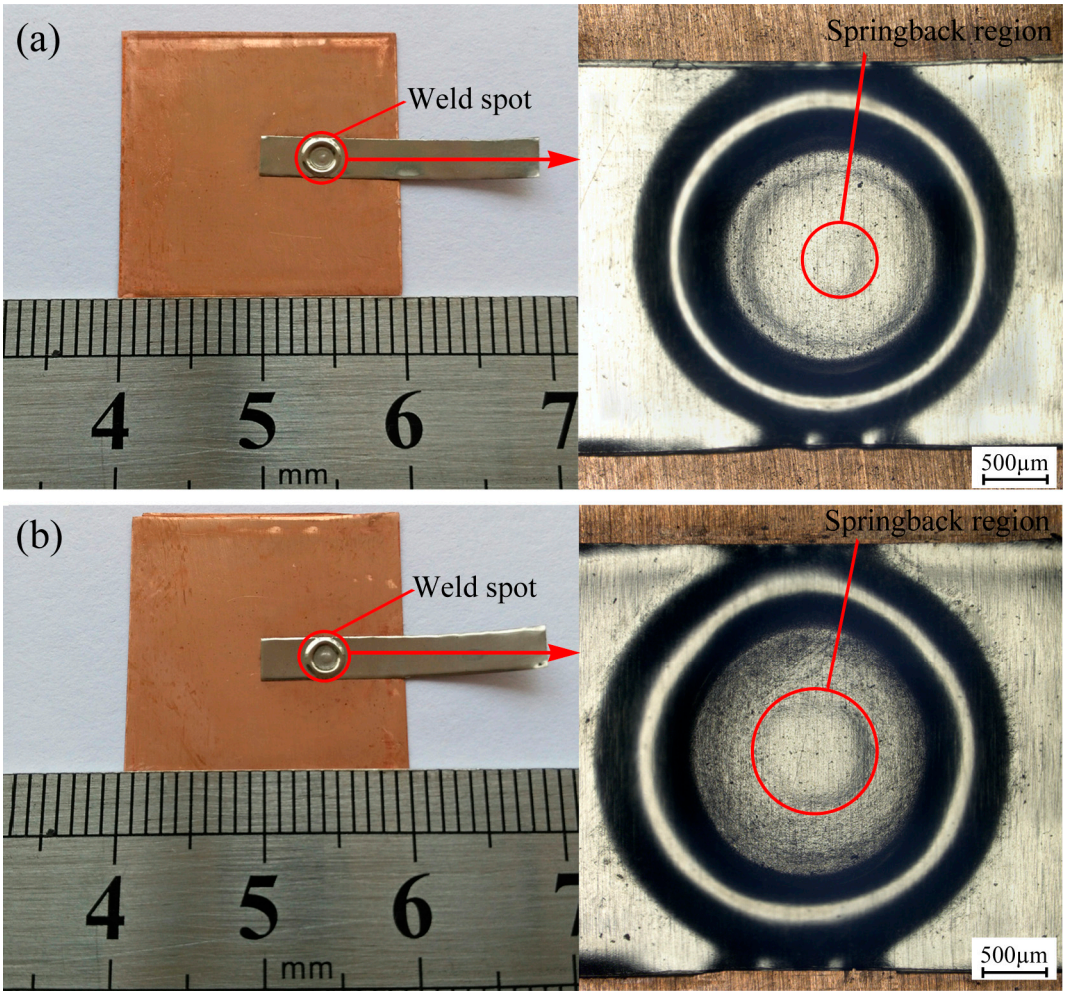

Figure 4. Weld samples and weld spots morphology from the laser impact spot welded joints at different laser pulse energies: (**a**) 565 mJ; (**b**) 1550 mJ.

Figure 5 presents the optical micrographs of the cross-section view of Ti/Cu joints shown in Figure 4. Annular bonding region was observed. When the hump hit the base plate, the collision angle between the hump and the base plate was less than the critical angle at the initial collision stage, so bonding did not occur in the central region of the weld spots. Consequently, an annular bonding region was formed after the LISW. It can be noted from Figure 5 that the area of the bonding region increased when the pulse energy increased from 565 mJ to 1550 mJ. The area was measured to be about 0.34 mm^2 and 0.88 mm^2, respectively. The reason why the area of the bonding region became larger with the increase of pulse energy may be expressed as follows: as the pulse energy increases, the maximum impact velocity also goes up, which leads to the increase of the scope of effective impact velocity.

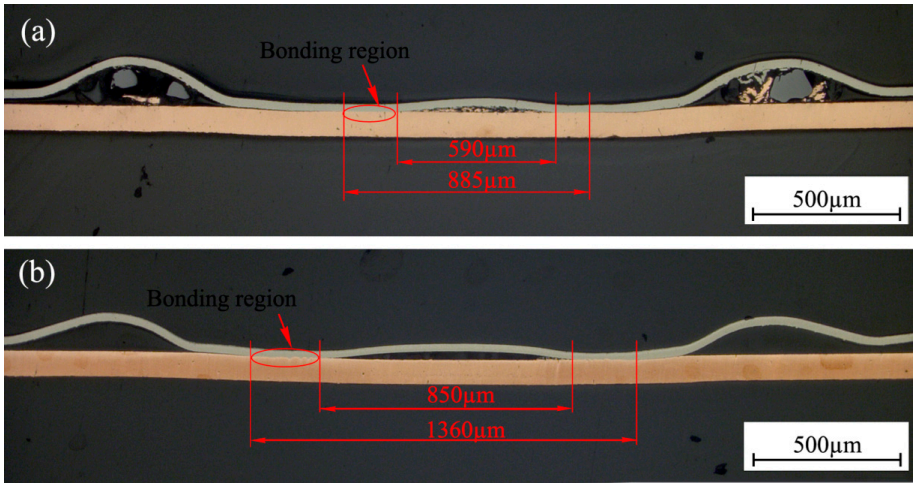

Figure 5. Optical micrographs of the cross-section view of Ti/Cu joints produced at different laser pulse energies: (**a**) 565 mJ; (**b**) 1550 mJ.

4.2. Microstructure

Figure 6 presents the microstructure of the Ti/Cu joint produced at 1200 mJ pulse energy. Figure 6a shows an overview of SEM morphology of the weld cross-section. It is interesting that entrapped jetting was observed in the center of the weld spot as shown in Figure 6c. When the hump on the flyer plate (Ti) bulged and obliquely impacted the base plate (Cu), a high velocity jet which contained oxidized surface layer, contaminants, and a thin layer of metals was generated at the collision point. Then two clean and fresh surfaces were formed and brought into atomic distance by laser induced shockwave pressure. As a result, bonding was obtained [22]. Moreover, most of the researchers believed that the jet must be present in the welding process in order to achieve successful welding [23–25]. So, it is suggested that jetting formation was one of the conditions for the occurrence of LISW of Ti and Cu.

Normally, two morphologies can be achieved—flat and wavy [14,16–19]—when the LIW has happened. Generally, a wavy weld interface is expected because this interface can increase the bonding area and assist interlocking between two metal surfaces [14] as shown in Figure 6b,d. Similar interface morphology was also found at other pulse energies (565 mJ, 835 mJ, and 1550 mJ). Both wave length and amplitude of the waves varied gradually along the weld interface as shown in Figure 6a,d. These wave interface features were also observed in high projectile impact spot welding and water jet spot welding [27,28]. Similar wave interface was also reported by Bahrani et al. [22] for explosive welding a flat flyer plate to a semi-cylindrical parent plate. It was found that welding did not happen when the collision angle was in the range of 0°–6°, however, welding with wave weld interface was obtained when the collision angle was in the range of 6°–20°. Vivek et al. [9] welded Ti sheets to grooved Cu targets by VFAW and found that welding with wave morphology occurred when the collision angle was in the range of 8°–20° with appropriate impact speed. The wave weld interface also indicates that the parameters selected in this study is reasonable based on the above analysis.

From Figure 6e,f, it can be seen that the weld interface close to the unbonded region was pulled apart. This result is the same with the finding presented by Wang's research for the welding of aluminum and titanium [19]. One way that this phenomenon could be explained as follows: At the initial phase of bonding between Ti and Cu, the bonding strength of the weld interface is relatively low due to the low collision angle (below 8°) between the hump and base plate. Then, under the drag effect of the springback of the hump, the weak weld interface is pulled apart.

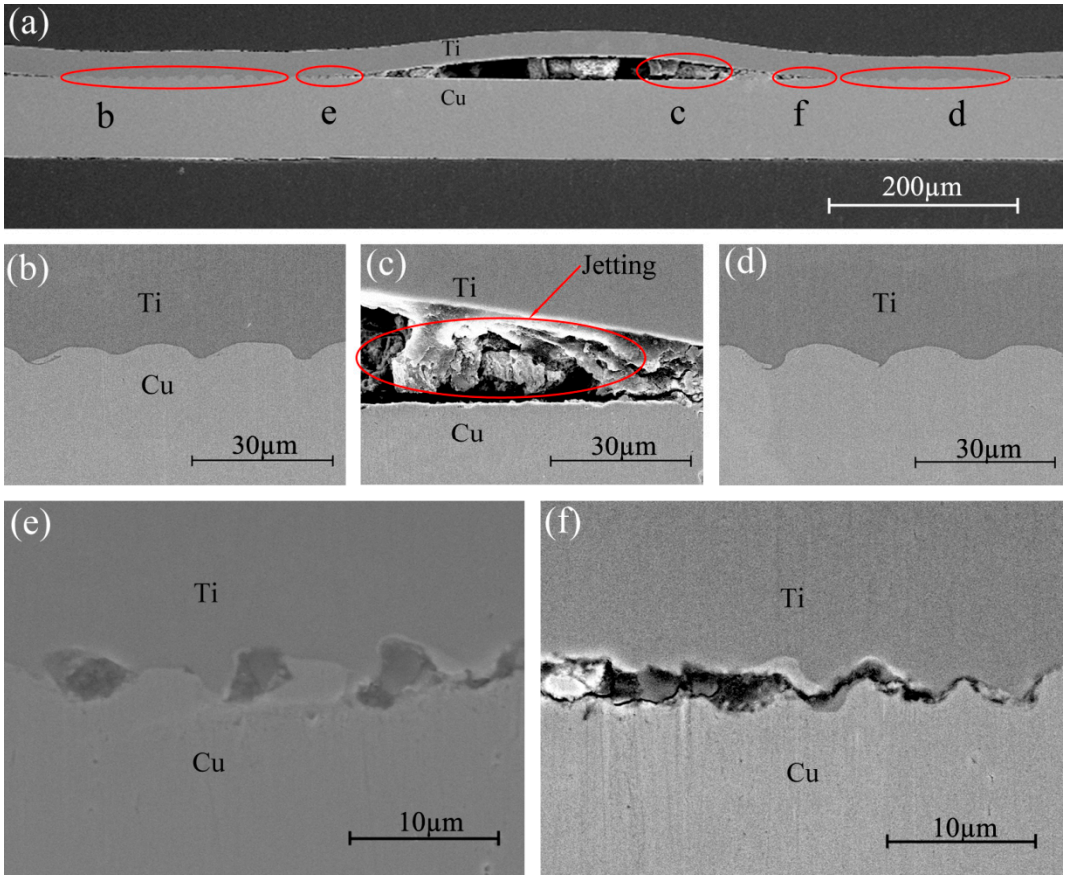

Figure 6. Microstructure of the weld interface of Ti/Cu joint produced at 1200 mJ pulse energy: (**a**) overview of cross-section of the weld between Ti and Cu, (**b**–**d**) magnified views of regions b-d marked in (**a**).

In the present laser impact spot welding approach, laser induced shockwave pressure deformed the hump on the flyer plate. Then the bulged hump was forced to impact toward the base plate at a high velocity. Figure 7 schematically illustrates the formation process of the spot welded joint. In the experiments, the central region of the hump was irradiated by much higher laser energy because the laser beam is subject to Gaussian distribution. Thus, much higher laser induced shockwave pressure is produced at this region, which contributed to the hump bulging and colliding onto the base plate at a high speed as shown in Figure 7b. During the impact phase, theoretically, the hump contacts the base plate first at 0° as shown in Figure 7c, and bonding did not happen. As the collision point moved from the center of the weld spot to the outside along the radius direction, the collision angle (α) between the hump and the base plate gradually increased. When it reached a certain value (about 8°) bonding took place with wave morphology between the hump and the base plate as shown in Figure 7d. The welding process continued until the collision angle exceeded the threshold (about 20°). Consequently, the laser impact spot welded joint was accomplished with an annular bonding region as shown in Figure 7e.

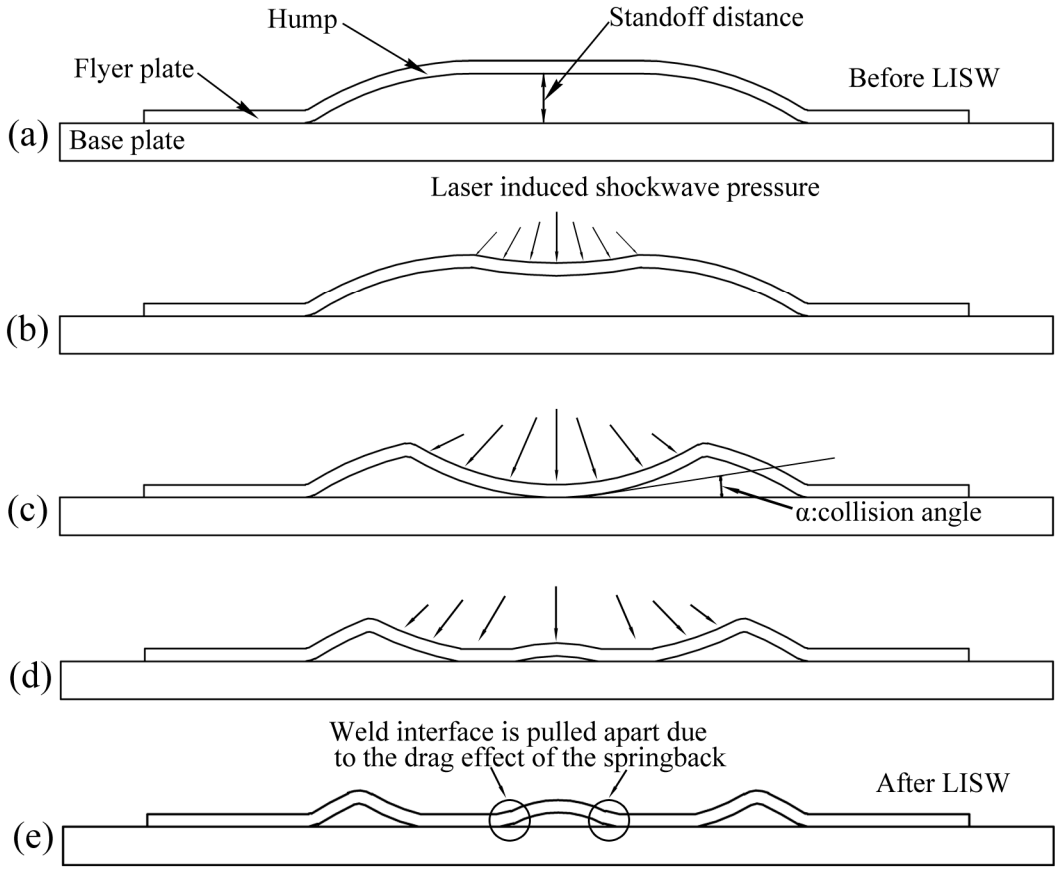

Figure 7. Schematic illustration for the formation process of the laser impact spot welded joint. (**a**) before LISW; (**b**) the hump bulges and collides onto the base plate at a high speed; (**c**) the hump contacts the base plate first at 0°; (**d**) welding phase; (**e**) after LISW.

SEM micrographs in Figure 8 display the differences in the weld interfaces of the spot welded Ti/Cu joints using different pulse energies. When 565 mJ and 835 mJ pulse energies were utilized, the wave length and amplitude of the interfacial waves were relatively small compared with others shown in Figure 8a,b. This may be the result of low pulse energy. Additionally, it was observed that the wave length and amplitude of the interfacial waves increased with the increase of pulse energy as shown in Figure 8a–d. The occurrence of this phenomenon may be because plastic deformation increased in the weld interface with the increase of pulse energy. Kahraman and Gülenç [6] found similar phenomenon in explosive welding of copper plates to titanium plates. They stated that plastic deformation increased in the weld interface with the increase of explosive energy, leading to the increase of wave length and amplitude. Similar results were also reported by Vivek et al. [9]. Besides, the increase of deformation in the interface may also result in increased hardness near the weld interface of the spot welded Ti/Cu joints [6].

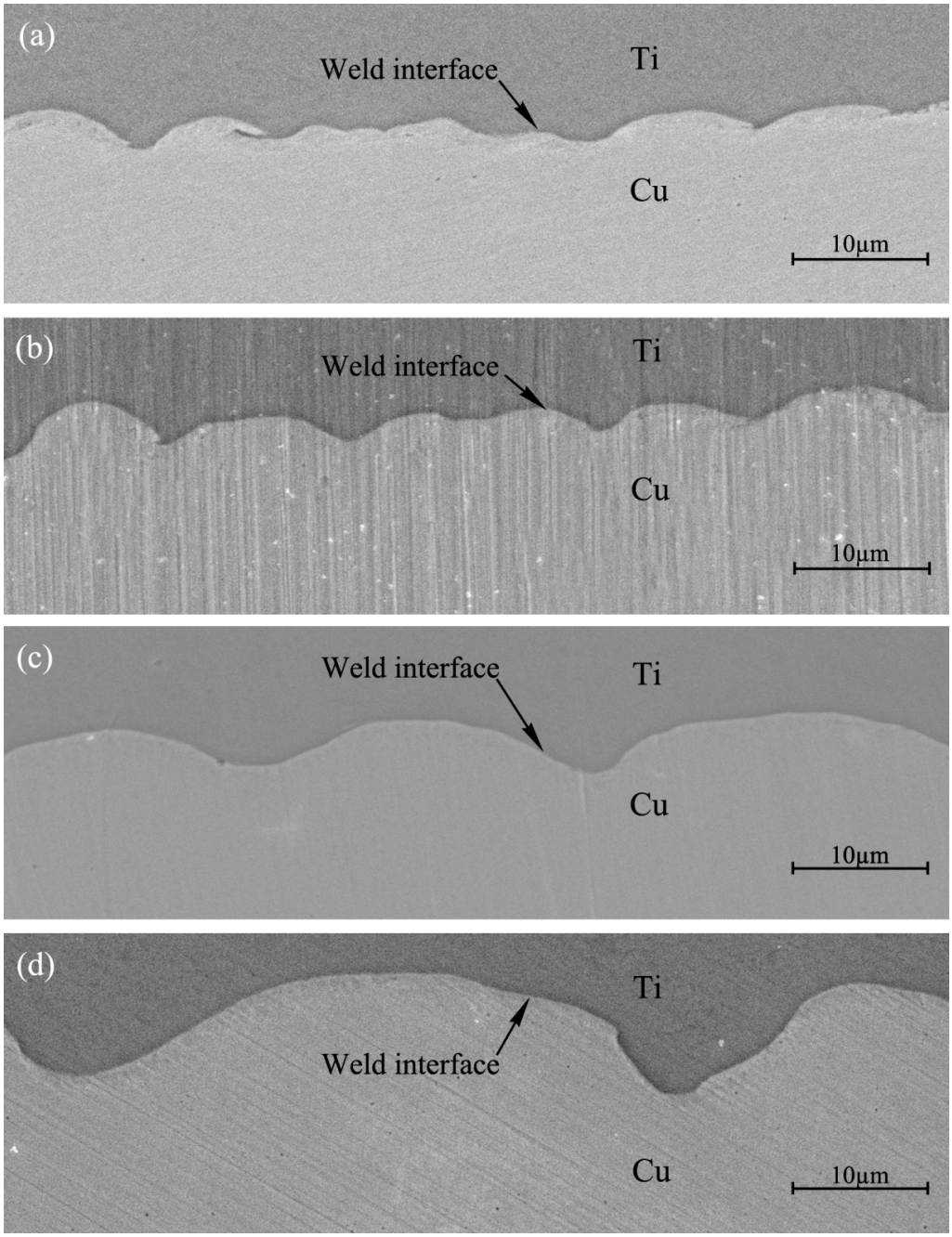

Figure 8. SEM micrographs of the weld interfaces obtained at different pulse energies: (**a**) 565 mJ; (**b**) 835 mJ; (**c**) 1200 mJ; (**d**) 1550 mJ.

From Figure 8, sharp weld interfaces also can be observed clearly. It is interesting to point out that intermetallic phases did not occur at the weld interfaces. This finding was -consistent with the previous reports [6,17–19]. It may be because the impact velocity of the hump is relatively low compared with the explosive welding, the heat resulting from the impact energy is also relatively small. In turn, the increase of the temperature of the interfacial material is too small to reach the melting point of Ti and Cu [17]. The results of the EDS line scanning across Cu, weld interface, and Ti confirm the above statement, as shown in Figure 9. In Figure 9b, the "TiK" and "CuK" means K line of titanium and copper, respectively. The red and green curves indicated the changes of element content of Ti and Cu, respectively. It can be seen that element content (Cu and Ti) varied sharply in the weld interface. The result showed that apparent element diffusion did not occur across the weld interface. In the

LISW process, laser induced shockwave pressure can reach several GPa, but the peak pressure is only maintained for a few nanoseconds [21]. Accordingly, element diffusion occurs with difficulty in the LISW of Ti and Cu. Works from Wang et al. [19] confirmed the finding.

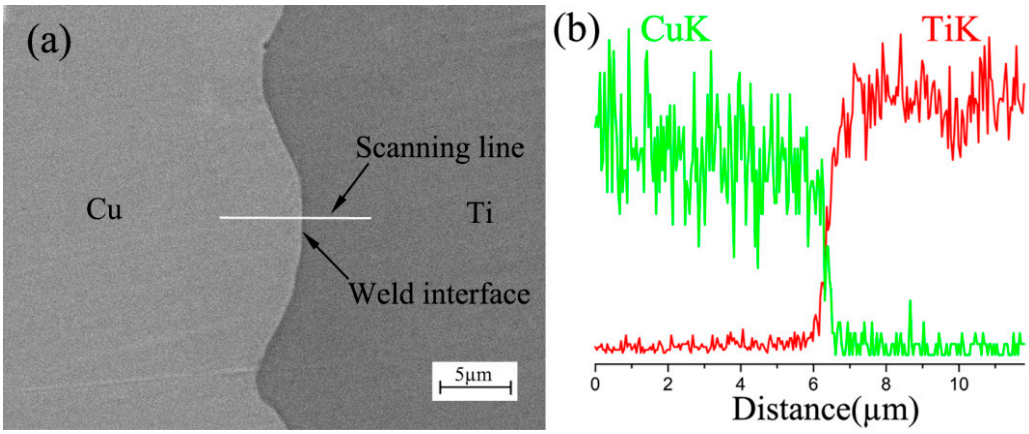

Figure 9. Energy dispersive spectroscopy (EDS) line scans across Cu, weld interface, and Ti of Ti/Cu weld spot produced at pulse energy of 1200 mJ: (**a**) SEM image; (**b**) elements distribution.

4.3. Lap Shearing Test

Lap shearing test was carried out to evaluate the bonding strength of the spot welded joints made at different pulse energy. The test setup is illustrated in Figure 10 corresponding to Figure 4. The tests were performed three times for each condition (565 mJ, 835 mJ, 1200 mJ, and 1550 mJ pulse energies). The average load was found out to be 14 N, 24 N, 28 N, and 30 N, respectively, when four kinds of pulse energy were utilized. The load (F) and displacement were recorded during tests as shown in Figure 11. It can be seen that the failure load of the joints increased with the increase in pulse energy. The increase in failure load might be because the bonding region gets larger with the increase in pulse energy as indicated in Figure 4. In addition, the wave length and amplitude of the weld interfaces increased with increased pulse energy as indicated in Figure 8, resulting in the increase of intimate contact area between Ti and Cu surfaces [14]. It also may be the reason for the increase of failure load. In addition, a large wave amplitude formed at high pulse energy can improve the effect of interlocking between two metal surfaces, which may enhance the tensile strength [6]. It was also noticed from Figure 11 that curve "a" and curve "b" had the same trend. Curve "c" and "d" also had the same trend. This finding may be related to the failure mode of the joints.

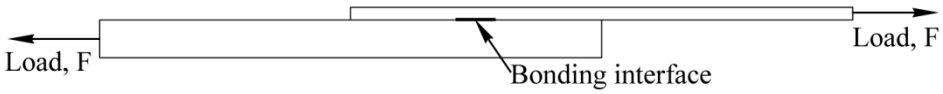

Figure 10. Illustration of lap shearing test.

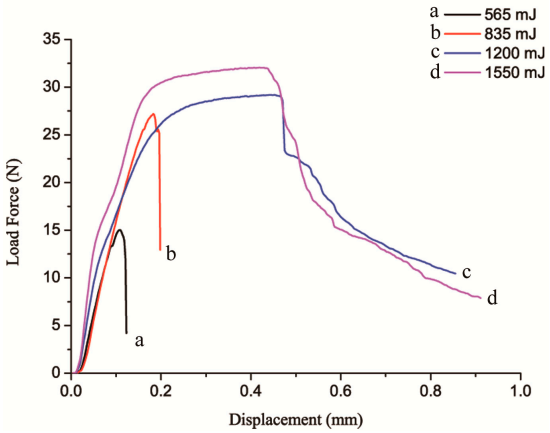

Figure 11. Force-displacement curves of spot welded samples produced at different pulse energy.

Generally, there were two different kinds of failure modes that were observed in the lap shearing test, as shown in Figure 12. Samples welded at 565 mJ or 835 mJ pulse energy failed on the bonding region after lap shearing tests, as shown in Figure 12a. This failure mode was interfacial failure. Furthermore, Figure 13 shows the SEM morphology of fracture surface of the base plate shown in the Figure 12a. A wavy appearance was observed on the bonding region, which can indicate the wave. The average shearing area (A) was measured to be 0.34 mm^2 and 0.47 mm^2 after lap shearing tests, respectively. The joint strength (MPa) was calculated by load divided by the shearing area (F/A). Accordingly, the shear strength of the joints welded with 565 mJ and 835 mJ pulse energy was found to be 41.2 MPa and 51.1MPa. It is possible that the low strength of the bonding region results in interfacial failure. Moreover, it was found that the shear strength with low pulse energy was higher than that reported by Wang et al. [16]. It indicates that bonding strength is related to interfacial morphology, and aa wavy interface is better than a flat interface because of the interlocking and increase in bonding area due to the waves [29].

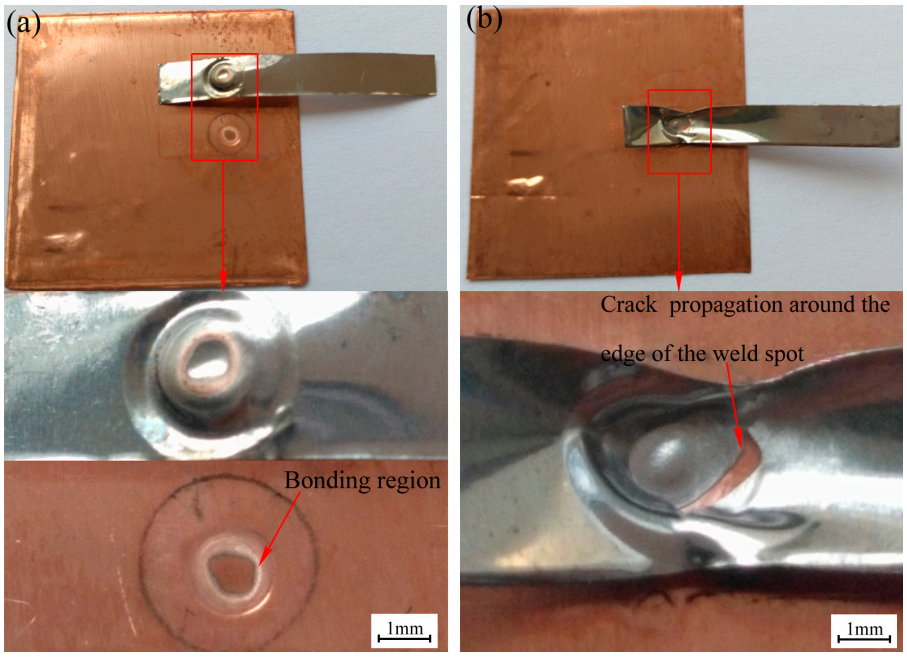

Figure 12. Failure modes of the spot welded specimens made with different pulse energies: (**a**) failure occurred on the bonding region after lap shearing test (835 mJ); (**b**) failure occurred along the edge of the weld spot after lap shearing test (1200 mJ).

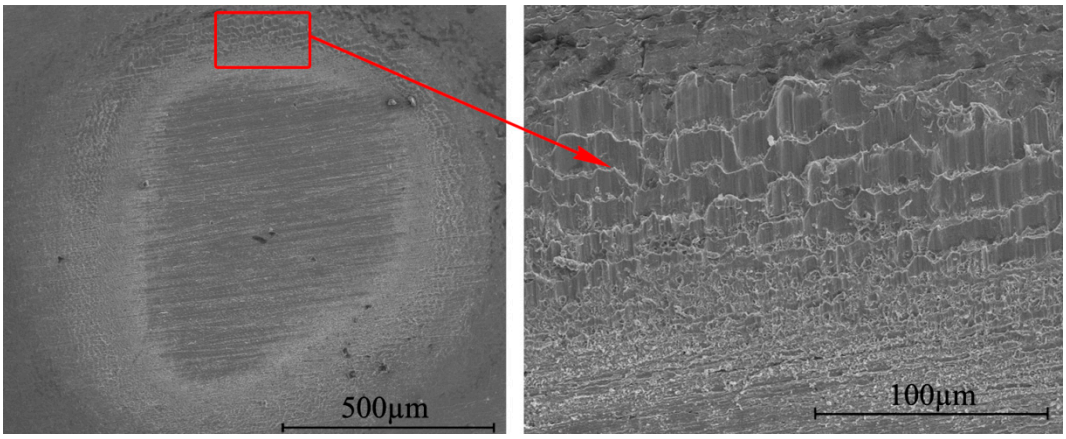

Figure 13. Fracture surface morphology on the base plate of the joint produced at 835 mJ pulse energy.

Nevertheless, the specimens fractured at the edge of the weld spots on the flyer plates after lap shearing tests when 1200 mJ and 1550 mJ pulse energy was applied shown in Figure 12b; this was pullout fracture mode. The crack propagation was found along the edge of the weld spot. The failure of the welded foils near the edge of the weld spot can be due to two reasons. Firstly, and most importantly, the stress concentrates around the edge of the weld spot during the lap shearing test. Secondly, during the pre-forming of the foil before welding, the bump of the foil was probably weakened due to the fact of foil thinning.

5. Conclusions

In this study, a novel laser impact spot welding method was developed. A standoff distance which is required between the flyer plate and the base plate in LIW was avoided in this method by use of local pre-forming on the flyer plate to form a "hump". The feasibility of this approach was verified by joining thin Ti foils to Cu foils with a low laser energy system. The morphology of the welded spots was examined. The microstructure of laser impact spot welded Ti/Cu joint was investigated. In addition, the mechanical properties of welded joints were studied. The following conclusions were made:

(1) Thin TA2 titanium foils and T2 copper foils were successfully welded by LISW. The joints with regular shape and high surface quality were obtained because only local plastic deformation occurred on the humps on the Ti plates during LISW. With the increase of pulse energy, annular bonding area was improved.

(2) Jetting was observed and was one of the conditions required for the occurrence of LISW of Ti and Cu. Wave characteristics were observed in the weld interface. Wave length and amplitude in the weld interface increased with increased impact energy.

(3) Intermetallic phases were not found in the weld interfaces based on the SEM micrographs. EDS analysis did not show apparent element diffusion across the weld interface.

(4) The failure load of the joints increased with the increase in laser energy. Two different types failure mode were observed. Samples welded by 565 mJ or 835 mJ pulse energy all failed in the bonding region. Specimens failed along the edge of the weld spots when 1200 mJ or 1550 mJ pulse energy was used.

Acknowledgments: This work is supported by the National Natural Science Foundation of China (No. 51175235) and Jiangsu University Students' Scientific Research Project (No. 15A025).

Author Contributions: Huixia Liu and Shuai Gao conceived and designed the experiments; Liyin Li, Cong Li and Xianqing Sun performed the experiments; Zhang Yan, Zongbao Shen, Chaofei Sha and Youjuan Ma analyzed the data; Huixia Liu, Shuai Gao and Xiao Wang wrote the paper.

Conflicts of Interest: The authors declare no conflict of interest.

References

1. Cao, R.; Feng, Z. Microstructures and properties of titanium-copper lap welded joints by cold metal transfer technology. *Mater. Des.* **2014**, *53*, 192–201. [CrossRef]
2. Hosseini, M.; Manesh, H.D. Bond strength optimization of Ti/Cu/Ti clad composites produced by roll-bonding. *Mater. Des.* **2015**, *81*, 122–132. [CrossRef]
3. Chen, G.Q.; Zhang, B.G. Influence of electron-beam superposition welding on intermetallic layer of Cu/Ti joint. *Trans. Nonferrous Met. Soc. China* **2012**, *22*, 2416–2420. [CrossRef]
4. Shiue, R.K.; Wu, S.K. The interfacial reactions of infrared brazing Cu and Ti with two silver-based braze alloys. *J. Alloy. Compd.* **2004**, *372*, 148–157. [CrossRef]
5. Lee, J.G.; Kim, G.H. Intermetallic formation in a Ti-Cu dissimilar joint brazed using a Zr-based amorphous alloy filler. *Intermetallics* **2010**, *18*, 529–535. [CrossRef]
6. Kahraman, N.; Gülenç, B. Microstructural and mechanical properties of Cu-Ti plates bonded through explosive welding process. *J. Mater. Process. Technol.* **2005**, *169*, 67–71. [CrossRef]
7. Meshram, S.D.; Mohandas, T. Friction welding of dissimilar pure metals. *J. Mater. Process. Technol.* **2007**, *184*, 330–337. [CrossRef]
8. Aydın, K.; Kaya, Y. Experimental study of diffusion welding/bonding of titanium to copper. *Mater. Des.* **2012**, *37*, 356–368. [CrossRef]
9. Vivek, A.; Liu, B.C. Accessing collision welding process window for titanium/copper welds with vaporizing foil actuators and grooved targets. *J. Mater. Process. Technol.* **2014**, *214*, 1583–1589. [CrossRef]
10. Daehn, G.S.; Lippold, J.C. Low Temperature Spot Impact Welding Driven without Contact. U.S. Patent PCT/US09/36299, 6 January 2011.
11. Findik, F. Recent developments in explosive welding. *Mater. Des.* **2011**, *32*, 1081–1093. [CrossRef]
12. Kore, S.D.; Date, P.P. Effect of process parameters on electromagnetic impact welding of aluminum sheets. *Int. J. Impact Eng.* **2007**, *34*, 1327–1341. [CrossRef]
13. Hahn, M.; Weddeling, C. Vaporizing foil actuator welding as a competing technology to magnetic pulse welding. *J. Mater. Process. Technol.* **2016**, *230*, 8–20. [CrossRef]
14. Zhang, Y.; Babu, S.S. Application of high velocity impact welding at varied different length scales. *J. Mater. Process. Technol.* **2011**, *211*, 944–952. [CrossRef]
15. Wang, H.; Liu, D.; Taber, G. Laser Impact Welding-Process Introduction and Key Variables. Available online: https://eldorado.tu-dortmund.de/bitstream/2003/29542/6/Wan12.pdf (accessed on 27 July 2016).
16. Wang, X.; Gu, C.X. Laser shock welding of aluminum/aluminum and aluminum/copper plates. *Mater. Des.* **2014**, *56*, 26–30. [CrossRef]
17. Wang, X.; Gu, Y.X. An experimental and numerical study of laser impact spot welding. *Mater. Des.* **2015**, *65*, 1143–1152. [CrossRef]
18. Wang, H.; Taber, G. Laser impact welding: Design of apparatus and parametric optimization. *J. Manuf. Process.* **2015**, *19*, 118–124. [CrossRef]
19. Wang, H.; Vivek, A. Laser impact welding application in joining aluminum to titanium. *J. Laser Appl.* **2016**, *28*, 032002-1–032002-7. [CrossRef]
20. Montross, C.S.; Wei, T. Laser shock processing and its effects on microstructure and properties of metal alloys: A review. *Int. J. Fatigue* **2002**, *24*, 1021–1036. [CrossRef]
21. Liu, H.X.; Shen, Z.B. Numerical simulation and experimentation of a novel micro scale laser high speed punching. *Int. J. Mach. Tool. Manuf.* **2010**, *50*, 491–494. [CrossRef]
22. Bahrani, A.S.; Black, T.J.; Crossland, B. The mechanics of wave formation in explosive welding. *Proc. Royal Soc. Ser. A* **1967**, *296*, 123–136. [CrossRef]
23. Mousavi, A.A.A.; Al-Hassani, S.T.S. Numerical and experimental studies of the mechanism of the wavy interface formations in explosive/impact welding. *J. Mech. Phys. Solids* **2005**, *53*, 2501–2528.
24. Wang, X.; Zheng, Y. Numerical study of the mechanism of explosive/impact welding using smoothed particle hydrodynamics method. *Mater. Des.* **2012**, *35*, 210–219. [CrossRef]

25. Sapanathan, T.; Raoelison, R.N. Depiction of interfacial characteristic changes during impact welding using computational methods: Comparison between Arbitrary Lagrangian-Eulerian and Eulerian simulations. *Mater. Des.* **2016**, *102*, 303–312. [CrossRef]
26. EN ISO 527-1:2012. Plastics-determination of tensile properties—Part 1: General principles. Available online: https://www.iso.org/obp/ui/#iso:std:iso:527:-1:ed-2:v1:en (accessed on 27 July 2016).
27. Turgutlu, A.; Al-hassani, S.T.S. Experimental investigation of deformation and jetting during impact spot welding. *Int. J. Impact Eng.* **1995**, *16*, 789–799. [CrossRef]
28. Chizari, M.; Al-hassani, S.T.S. Experimental and numerical study of water jet spot welding. *J. Mater. Process. Technol.* **2008**, *198*, 213–219. [CrossRef]
29. Zhang, Y.; Babu, S.S. Microstructure characterisation of magnetic pulse welded AA6061-T6 by electron backscattered diffraction. *Sci. Technol. Weld. Join.* **2008**, *13*, 467–471. [CrossRef]